Journal of Biomedical Optics

SPIEDigitalLibrary.org/jbo

Accurate *in situ* measurement of complex refractive index and particle size in intralipid emulsions

Miao L. Dong
Kashika G. Goyal
Bradley W. Worth
Sorab S. Makkar
William R. Calhoun
Lalit M. Bali
Samir Bali

SPIE

Accurate *in situ* measurement of complex refractive index and particle size in intralipid emulsions

Miao L. Dong,[a*] Kashika G. Goyal,[a*] Bradley W. Worth,[a] Sorab S. Makkar,[a] William R. Calhoun,[b] Lalit M. Bali,[a] and Samir Bali[a]
[a]Miami University, Department of Physics, Oxford, Ohio 45056
[b]U.S. Food and Drug Administration, Center for Devices and Radiological Health, Silver Spring, Maryland 20993

Abstract. A first accurate measurement of the complex refractive index in an intralipid emulsion is demonstrated, and thereby the average scatterer particle size using standard Mie scattering calculations is extracted. Our method is based on measurement and modeling of the reflectance of a divergent laser beam from the sample surface. In the absence of any definitive reference data for the complex refractive index or particle size in highly turbid intralipid emulsions, we base our claim of accuracy on the fact that our work offers several critically important advantages over previously reported attempts. First, our measurements are *in situ* in the sense that they do not require any sample dilution, thus eliminating dilution errors. Second, our theoretical model does not employ any fitting parameters other than the two quantities we seek to determine, i.e., the real and imaginary parts of the refractive index, thus eliminating ambiguities arising from multiple extraneous fitting parameters. Third, we fit the entire reflectance-versus-incident-angle data curve instead of focusing on only the critical angle region, which is just a small subset of the data. Finally, despite our use of highly scattering opaque samples, our experiment uniquely satisfies a key assumption behind the Mie scattering formalism, namely, no multiple scattering occurs. Further proof of our method's validity is given by the fact that our measured particle size finds good agreement with the value obtained by dynamic light scattering. [DOI: 10.1117/1.JBO.18.8.087003]

Keywords: turbid media; refractive index; scattering media; optical tissue; intralipid.

Paper 130396R received Jun. 6, 2013; revised manuscript received Jul. 2, 2013; accepted for publication Jul. 3, 2013; published online Aug. 7, 2013.

1 Introduction

The measurement of optical properties of biological tissue, or tissue-like turbid media, has received considerable attention, with various novel methodologies being proposed and demonstrated.[1–21] Here, "turbid" refers to a colloidal suspension of light-scattering oil droplets of size comparable to the optical wavelength. For the purpose of instrument calibration, and the validation of theoretical predictions on light–tissue interaction, researchers have developed "phantoms"—artificial media that simulate the optical properties of tissue.[22–27] This "optical tissue" is stable, reproducible, easily prepared, readily accessible, and far simpler to model than actual biological tissue. The most widely used medium for phantom preparation is a fat emulsion, i.e., a highly turbid aqueous suspension of oil droplets, commonly used as a human intravenous nutrient, that goes by any one of the trade names intralipid, nutralipid, or liposyn.

It is noteworthy that, despite all the attention, a precise *in situ* determination of several important optical properties of intralipid emulsions, such as the particle size, refractive index, and attenuation coefficient (which is commonly expressed as the imaginary part of a complex refractive index[13–21]), has continued to elude researchers.[28] The chief difficulty arises from the fact that intralipid emulsions, being highly turbid, have a large attenuation coefficient. From the point of view of particle sizing, standard methods such as optical microscopy and dynamic light scattering (DLS) require heavy sample dilution and are hence not *in situ*. Dilution inevitably leads to errors and, hence, wide variations in measured particle size. For example, reports of measurements of the average particle diameter in intralipid and liposyn have ranged anywhere from 97 nm (Ref. 26) to 185 nm (Ref. 25) to values between 350 and 660 nm.[23,24,27] Clearly particle sizing in intravenous nutrients is critically important in order to eliminate the possibility of thrombosis.[23,28] From the point of view of *in situ* complex refractive index measurement of highly attenuating tissue, it is attractive to consider reflectance-based methods since very little light transmits through. However, the most widely used reflectance-based method, which equates the point of maximum slope of the reflectance-versus-incident-angle curve with an effective critical angle,[3,13–15,21] has been shown to be significantly inaccurate even after error-correction is attempted.[29] Other attempts to extract the complex refractive index by modeling the reflectance data either introduce extraneous fitting parameters (beyond the two parameters of interest, namely, the real and imaginary parts of the refractive index) resulting in overfitting of the data[19,20] or focus on only the critical angle region, which is just a small subset of the reflectance data.[14–18]. Both approaches have built-in arbitrariness causing wide variation in extracted values. Finally, note that the particle size is typically extracted from a measurement of the complex refractive index using a Mie calculation. A critical assumption for standard Mie theory to be valid is that no multiple scattering occurs.[30] For a highly turbid medium such as an intralipid emulsion, this criterion is only well satisfied when the sample length is no more than a micron (for

*Miao L. Dong and Kashika G. Goyal contributed equally to this work.

Address all correspondence to: Samir Bali, Miami University, Department of Physics, Oxford, Ohio 45056. Tel: 513-529-5635; Fax: 513-529-5629; E-mail: balis@miamioh.edu

light in the 400- to 1100-nm regime), a condition not met in previous work with intralipids to the best of our knowledge.

For all the above reasons, there is a wide variation in measured optical properties of highly attenuating media and a lack of consensus exists among researchers about which of the various methodologies referred to above[1–21] ought to be used as the gold standard for the optical characterization of tissue-like turbid media. The defining characteristics for a gold standard method are given in Ref. 7. The measurement is fast, *in situ*, amenable to calibration with readily available standard materials, usable over a wide spectral range, and described by a well-justified theoretical model that enables verifiably accurate extraction of the relevant optical parameters from the data. However it has been noted, for example, in Ref. 6 while comparing the works in Refs. 1, 4, 7, and 12, that "it seems difficult to find measurements with accuracy better than 10% even when measurements are carried out on homogeneous media in the most favorable experimental conditions." The authors in Ref. 6 also state that a comparison between the different methodologies reported in the literature is meaningless since the true value of the relevant optical property remains unknown. This is especially true for the refractive index and attenuation coefficient of optical tissue. For the same reason, the error reported in a specific methodology in previous works (for example, Refs. 4, 7, and 12) is an indication of the experiment's reproducibility, not departure from a true value.

Here we demonstrate a first accurate *in situ* measurement of the complex refractive index of an undiluted intralipid emulsion and deduce the average particle size of the suspended oil droplets using a Mie calculation. Our method employs a real-time sensitive measurement of total internal reflection (TIR) of a divergent laser beam from the sample surface, over the full range of incident angles, i.e., for reflectivity values going from unity in the TIR regime to nearly zero in the non-TIR regime where almost all the light is transmitted. We employ a new empirical model we introduced earlier[16,17,18] that incorporates angle-dependent penetration of the incident light into the medium during TIR. However, in contrast to Refs. 16, 17, and 18 where a small subset of the reflectance curve was focused on and previous works[5,14,15,20] where just ~20 data points were fitted, here we fit the entire reflectance curve comprising ~1000 data points. In further contrast to previous works[5,19–21] we employ no other fitting parameters besides the two variables we seek to determine—the real and imaginary parts of the refractive index—thus avoiding ambiguity in the extracted values owing to overfitting. To the best of our knowledge, this is the first case where the entire reflectance-versus-incident-angle data-curve, spanning both TIR and non-TIR regimes, has been accurately described by a theoretical model for any highly turbid medium. Importantly, despite our intralipid sample being highly scattering, no multiple scattering occurs in our experiment. It is unclear if this key requirement for Mie theory to be applicable has been satisfied in previous works, but we show it to be well satisfied in our case. The validity of our own model is reinforced by comparing the particle size predicted by our model with DLS and finding good agreement. DLS, though not *in situ*, is otherwise well suited for particle sizing in stable intralipid samples where the act of dilution does not impact the particle size distribution. Of course, in contrast to our methodology, DLS offers no reliable information on the real and imaginary parts of the refractive index.

2 Experimental Setup

Our setup for measuring the reflectance profile from a turbid medium has been detailed previously.[31] The sample is placed on top of a glass prism and illuminated by a fiber-coupled diode laser of wavelength 660 nm, as shown in Fig. 1(a). The single-mode fiber yields a divergent TEM_{00} laser beam,

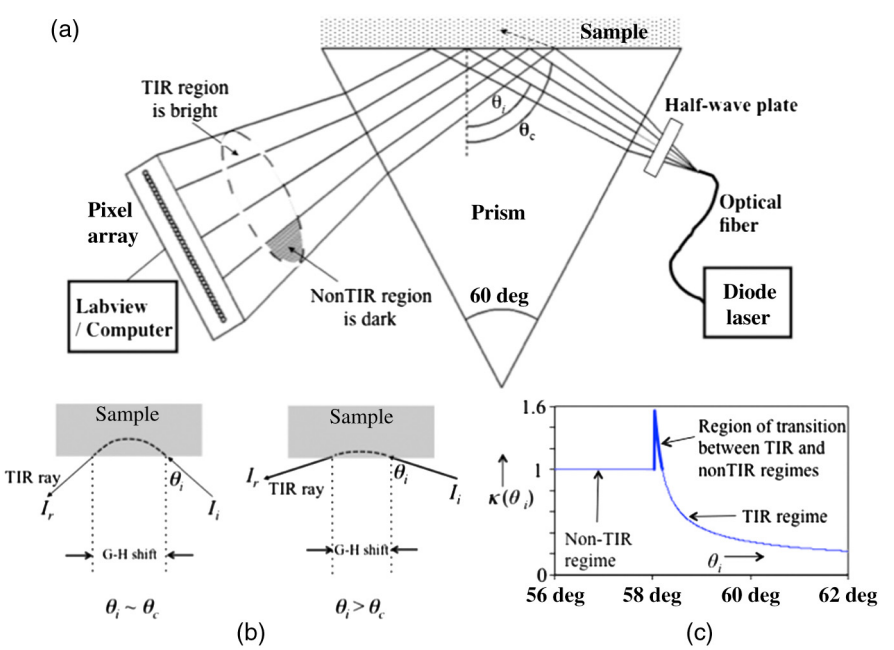

Fig. 1 (a) Schematic of experiment. The half-wave plate is used to adjust the linearly polarized fiber output as desired. For a transparent sample, the critical angle θ_c at which total internal reflection (TIR) first occurs manifests as a sharp edge within the reflected beam profile (the dashed ellipse shown). (b) Angle-dependent penetration of the incident light into a transparent medium during TIR, yielding the Goos-Hänchen shift δ_{GH}. In a turbid medium, θ_c is not well defined. (c) The angular-dependent component κ of $n_i(\theta_i)$, from Eq. (2); see text for explanation.

of angular half-width 7 deg, which is reflected from the prism–sample interface on to a one-dimensional pixel array (1024 pixels, each of diameter 14 μm). Only a central portion of the Gaussian beam-profile, spanning a full angular range of 8.2 deg, fits within the pixel array and is recorded. If the intensity reflected from the prism–sample interface is denoted as I_r and the intensity incident on the interface at angle θ_i is denoted as I_i, the angle-dependent reflectance profile $I_r/I_i(\theta_i)$ is measured by detecting the intensity readout from each pixel using Labview.[16,17,31] There is no angle-scanning required, in fact there are no moving parts at all, thus eliminating mechanical noise for all practical purposes. A careful analysis of optical and electrical noise in the system is presented in Ref. 31.

3 Our Theoretical Model

3.1 *Previous Work*

The theoretical model we employ to fit the reflectance data for turbid media was described in Refs. 16, 17, and 18—below we briefly recount its basic features. Next we describe two new insights, not previously mentioned in Refs. 16, 17, and 18, that are vitally important for enabling a first demonstration of reliable *in situ* particle sizing in intralipid emulsions.

Turbidity is quantitatively described by the attenuation coefficient α: $I(z) = I_0 e^{-\alpha z}$, where $I_z(I_0)$ is the intensity at z ($z = 0$). The refractive index n of the turbid sample is written as $n_r + in_i$, with the real part n_r describing the usual bending of light at the interface and the imaginary part n_i relating to the attenuation: $\alpha = 2n_i\omega/c$, where c is the speed of light in vacuum and ω is the laser frequency. For milk α is ~50 to 100 cm^{-1} at visible and near-infrared frequencies, and for biotissue α typically exceeds 200 cm^{-1}. Note that this traditional link between the attenuation α and the imaginary refractive index n_i is especially suited for perpendicular incidence (which is where most transmission-based experiments are carried out) or for incident angles less than the critical angle. For reflectance-based experiments in the TIR regime, one needs to re-examine this understanding of the imaginary refractive index.

The traditional approach to theoretically describing the reflectance for turbid media consists of simply allowing n_s to be complex in Fresnel theory, yielding for p-polarization.[16,17,21]

$$\frac{I_r}{I_i} = \frac{M + P^2\cos^2\theta_i - \sqrt{2}\,\cos\,\theta_i(M + \sin^2\theta_i)\sqrt{M + L}}{M + P^2\cos^2\theta_i + \sqrt{2}\,\cos\,\theta_i(M + \sin^2\theta_i)\sqrt{M + L}}, \tag{1}$$

where $P = (n_r^2 + n_i^2)/n_{\text{prism}}^2$, $L = [(n_r^2 - n_i^2)/n_{\text{prism}}^2] - \sin^2\theta_i$, and $M = \sqrt{P^2 - 2L\sin^2\theta_i - \sin^4\theta_i}$. In traditional Fresnel theory, n_i is treated as a constant for all incident angles. The problem with this approach is illustrated in Fig. 1(b), which also serves as the basis for our model described in Refs. 16 and 17. In TIR, the incident light ray penetrates the sample before coming back out at an exit point that is displaced with respect to the point of entry. This shift between the points of entry and exit was observed in 1947 and is referred to as the Goos-Hänchen shift.[32] The depth of penetration depends on the angle of incidence, as shown in Fig. 1(b), implying that the attenuation is angle-dependent and so is n_i. In Refs. 16 and 17 we showed that one may write this new angle-dependent $n_i(\theta_i)$ in terms of the traditional constant n_i as $n_i(\theta_i) = n_i\kappa(\theta_i)$, where the form for the angular factor κ is plotted in Fig. 1(c). From this figure we see that in the non-TIR regime, κ is set to be unity, and we recover the traditional constant n_i. However, in the TIR regime, κ is modeled as a smoothly varying downward sloping function given by[16,17]

$$\kappa(\theta_i) = \left[4\pi n_{\text{prism}}\sqrt{(M - L)/2}\right]^{-1}. \tag{2}$$

The spike appearing between the TIR and non-TIR regimes is discussed in Sec. 4.

Although progress has been made toward developing an accurate model of TIR in turbid media in Refs. 16, 17, and 18, an important shortcoming of these previous works is that the authors fit only the critical angle region (i.e., they fit the reflectance data between 0.75 and 1 while they ignored the reflectance data between 0 and 0.75). For this reason the authors in Refs. 16, 17, and 18 were in no position to perform particle sizing.

3.2 *New Insights*

Two new insights enable a first demonstration of reliable *in situ* particle sizing in intralipid emulsions.

The first insight arises by considering the question: Can Mie theory be used for particle sizing in highly turbid media? Multiple scattering seems inevitable in experiments with highly attenuating media. Standard Mie theory (i.e., with no corrections) is applicable only when single scattering events occur (i.e., an incident photon scatters from a particle in the turbid medium), but no multiple scattering occurs (i.e., the scattered photon must not scatter again).[30] However, note that in our experiment, the depth of penetration, which is angle-dependent, is exceedingly small, reaching a maximum of the order of a wavelength for incident angles near the TIR to non-TIR transition. Thus, the optical depth, defined as the product of the attenuation coefficient α and the sample length traversed (in our case, just the penetration depth) is much less than unity even for highly turbid media with α values up to 1000 cm^{-1}. For an intralipid emulsion we find in Sec. 4 that α is as high as 650 cm^{-1}. However, the sample length traversed is only $\tilde{\lambda}$, yielding an optical depth of just 0.05. This is the probability for an incident photon to be scattered. The probability for this photon to be rescattered goes at least as the square of 0.05. Therefore multiple scattering is negligible in our experiments, despite the high turbidity of intralipid, owing to the extremely small (λ) sample length traversed by the light. Note that multiple scattering is not negligible in transmission-based measurements even for a sample thickness as low as 0.1 mm, such as is used in state-of-the-art spectrophotometers.

The second insight addresses the question: What is the best procedure to most accurately fit the entire reflectance curve? The answer is obviously to fit as many datapoints as possible using as few fit-parameters as possible. The minimum number of fit-parameters is two, since the goal of the experiment is to determine the two unknowns n_r and n_i. The main insight here is that while fitting the maximum number of datapoints, it is important to break away from the mindset, brought on by previous work with transparent media, that the datapoints in the TIR to non-TIR transition region of the reflectance curve (where the critical angle occurs for transparent media) should have greater primacy bestowed on them than datapoints elsewhere on the curve. Breaking away from the old mindset results in an interesting twist to the data-fitting procedure—our model

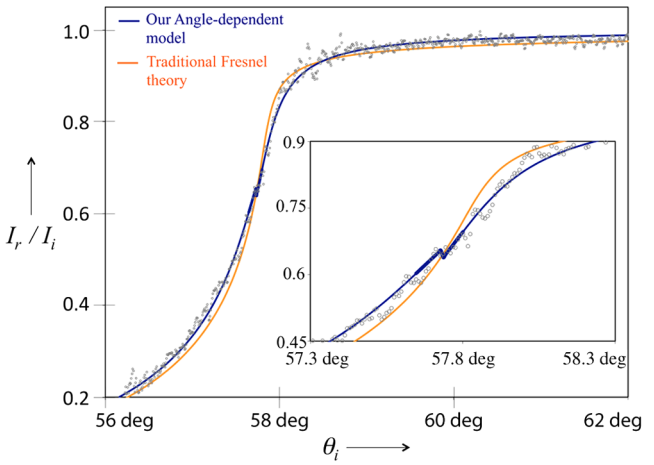

Fig. 2 The gray dots are reflectance data for intralipid 20%. Best fits obtained from our model (dark blue) and from conventional Fresnel theory (light orange) are shown. See text for an explanation of the kink (bold) in the fit from our model.

closely fits all parts of the reflectance curve (~1000 datapoints), yielding in the process a discontinuity in the fit over about ~20 datapoints that span the TIR to non-TIR transition region. This discontinuity causes the spike in Fig. 1, which is at first glance unsatisfactory to the eye. However, in Sec. 4 below we show that our new approach yields a first accurate *in situ* measurement of particle size and complex refractive index in intralipid emulsions.

4 Data and Discussion

Figure 2 shows I_r/I_i-curves as a function of incident angle θ_i for an undiluted sample of intralipid 20%. Intralipid 20% mainly consists of 20 g of soybean oil (n_r 1.47000, specific gravity 0.9190), which forms suspended droplets in 100 mL of water (n_r 1.33249 at 25°C) upon emulsification with egg lipid, causing turbidity. The egg lipid also forms small micelles of size approximately few nanometers, which do not contribute to turbidity. We seek to demonstrate an accurate *in situ* measurement (i.e., without sample dilution) of the complex refractive index and, subsequently, the average size of the suspended oil droplets.

The dark blue and light orange curves in Fig. 2 are best fits obtained from our angle-dependent model (AM) [Eqs. (1) and (2)] and traditional Fresnel (F) theory [Eq. (1) alone], respectively, by minimizing the mean squared deviation [MSD, defined as $(1/k)\sum_{i=1}^{k}(\text{observed value} - \text{predicted value})^2$, where k is the total number of datapoints being fitted] between the data and the model. Note that neither model employs extraneous fitting parameters, such as those used in previous work.[19,21] The only two fitting parameters used are the two unknowns that we seek to determine, i.e., n_r and n_i. (Owing to the extreme thinness of the penetration depth into the sample by the light (see Sec. 3.2) the density of scatterers encountered near the surface may be slightly different from the density that exists in the bulk.[20] A third fitting parameter may be employed to model the slight departure from the bulk value of the complex refractive index within a thin layer (of thickness equal to the particle diameter) at the surface, but we have chosen not to do so in this work.)

Once the complex refractive index is determined, the average particle size for the oil droplet may be determined from a numerical Mie calculation.[33] Assuming a particle size enables calculation of the scatterer density and, from the Mie program, the value of α. The particle size is varied until the program yields an α equal to our experimentally measured value. Note, from our discussion in the previous section that our experiment is perhaps the first instance in reported literature where standard Mie theory applies in highly turbid media.[30] Although both AM and F-models seem to fit the data about equally well, i.e., the MSD values shown in Table 1 for each model's fit are not too different, the table shows that the particle size extracted from either fit is significantly different. The table also shows that the predicted attenuation coefficients by either fit differ by more than a factor of two. Even the n_r values predicted by each fit differ by >0.001, which is significant for just about any cutting-edge application one can think of.

Three sets of data are taken, from which the error-bars indicated in Table 1 arise owing to statistical error. Systematic error also arises from the use of a divergent beam with a half waveplate but is far smaller than the statistical error and is therefore ignored: A ±4.1 deg departure from perpendicular incidence corresponds to a deviation in $\lambda/2$-shift of ±0.3% for the outermost rays of the divergent cone. We have checked that this leads to an uncertainty in our n_r and n_i values (and also particle size) that is an order of magnitude less than the statistical error bars indicated in the table.

The reason our model succeeds and traditional Fresnel theory fails is that, while the F-model uses constant n_i at all angles, our model switches between constant n_i in the non-TIR regime and angle-dependent $n_i(\theta_i)$ [see Fig. 1(c) and Eq. (2)] in the TIR regime. The spike in Figs. 1 and 2 results from the fact that in a highly attenuating medium the concept of a critical angle is untenable; hence one really does not know where the TIR regime ends and where the non-TIR regime begins. We overcome this problem by adopting the following four-step

Table 1 The mean size for the suspended oil droplets extracted from our angle-dependent model (AM) is drastically different from the size obtained from traditional Fresnel theory (F). The size error in the last column is the percentage error compared to the size obtained from dynamic light scattering (DLS). The two models also differ significantly in their predictions for n_r, n_i, and α. DLS yields 0.2962 μm for the particle size, within 7% of our result, but disagreeing with the F-model's prediction by almost 40%. Hence we trust our model's *in situ* sizing capability as well as its predictions for n_r, n_i, and α.

Model	n_r	$n_i(\times 10^{-4})$ (α in cm^{-1})	MSD ($\times 10^{-4}$)	Mean particle diameter (μm)	Sizing error relative to DLS
AM	1.36704 ± 0.00001	33.7 ± 0.3 (642 ± 5)	2.1	0.3175 ± 0.0019	7%
F	1.36704 ± 0.00001	13.3 ± 0.1 (254 ± 2)	4.1	0.1820 ± 0.0006	39%

fitting procedure. First, owing to the circular nature of Eqs. (1) and (2), we begin by inserting constant-value best-guesses for n_r and n_i in the expressions for L, M, and P in Eq. (1) and construct an angle-dependent $n_i(\theta_i)$ from Eq. (2). Second, as an initial location of the transition between the TIR and non-TIR regimes, we choose the angle at which the function $L(\theta_i)$ in Eqs. (1) and (2) changes sign from positive (non-TIR regime) to negative (TIR). The rationale for this starting choice is that $L(\theta_i)$ exhibits this same behavior for a transparent medium, i.e., in the $\alpha = 0$ case, L changes sign at the critical angle. Third, we substitute this new $n_i(\theta_i)$ back into Eq. (1) and perform a best fit of I_r/I_i to the data, where the only two fitting parameters we adjust are the very first best-guess values we used for n_r and n_i in step 1. Finally, we iteratively optimize n_r and n_i while simultaneously allowing the TIR to non-TIR transition point to vary around the initial location chosen in step 2. The iterations are continued until the MSD value is minimized—just a few iterations are required.

The origin of the kink in our theoretical fit (see inset in Fig. 2) is the fact that the fit in the non-TIR regime (where n_i is assumed to be constant) does not match up continuously with the fit in the TIR regime [where n_i has the angle dependence expressed in Eq. (2)]. However, the important point is that our model obtains unprecedented agreement with the entire reflectance data, spanning reflectivity values from one down to almost zero. This approach—whereby we obtain excellent agreement with a data set comprising ~1000 points while tolerating an ungainly discontinuity over a range of a few datapoints in the TIR to non-TIR transition region—is in stark contrast to the approach adopted by previous workers wherein all attention was focused on fitting just the critical angle zone.[14–18]

5 Conclusion

We have demonstrated a first accurate *in situ* measurement of the real refractive index, attenuation coefficient, and average scatterer-size in an intralipid emulsion. Because no sample dilution is required, our method has the potential to offer *in situ* long-term stability monitoring of lipid emulsions against the formation of potentially embolic fat globules larger than 5 μm owing to coalescence during on-shelf storage. An important open problem is the development of methods to directly measure the large-diameter tail of the globule size distribution. Here we have focused instead on the easier, though unresolved, problem of the precise measurement of the mean particle size. Such a measurement can, in principle, be made sensitive enough to detect a slight skewing in mean size caused by the presence of these large globules.

A word of caution is in order at the present time. We initially tested our theoretical model for TIR in a highly turbid medium [i.e., Eq. (2)] in milk-cream mixtures,[16,17,18] and now have performed a more rigorous test in intralipid emulsions. However, both milk and intralipid are polydisperse media for which no reference data exists on various optical parameters, including the complex refractive index and particle size. In order to convincingly test the validity of our model of angle-dependent penetration, we need to make extensive measurements in highly turbid monodisperse samples of various turbidities and particle sizes. Such measurements on aqueous solutions of polystyrene microspheres are in progress in our lab. Our model, once rigorously validated, may have implications for diverse applications—from modeling diffuse reflectors for light trapping enhancement in solar cells, where the reflectance at the glass–diffuse coating interface is poorly understood,[34,35] to verifying the occurrence of negative refractive index in novel nanoparticle-based metamaterials,[36] to enhancing the refractive index sensing capabilities of surface plasmon resonance-based techniques.[37]

Acknowledgments

We thank Mr. Lynn Johnson, formerly in the Miami University Instrumentation Lab, for Labview help. We are grateful to Mr. Michael Eldridge, former instrument maker in the Department of Physics at Miami University, for machining support. We acknowledge Ms. Sangeeta Singh for useful discussions on goodness-of-fit. We are indebted to the Petroleum Research Fund and Dillon-Kane, LLC, for financial support.

References

1. A. B. Pravdin, S. P. Chernova, and T. G. Papazoglou, "Tissue phantoms," Chapter 5 in *Handbook of Optical Biomedical Diagnostics*, V. V. Tuchin, Ed., pp. 311–352, SPIE Press, Bellingham, WA (2002).
2. R. Hennessey et al., "Monte Carlo lookup table-based inverse model for extracting optical properties from tissue-simulating phantoms using diffuse reflectance spectroscopy," *J. Biomed. Opt.* **18**(3), 037003 (2013).
3. Q. Ye et al., "Measurement of the complex refractive index of tissue-mimicking phantoms and biotissue by extended differential total reflection method," *J. Biomed. Opt.* **16**(9), 097001 (2011).
4. R. Saager, D. Cuccia, and A. Durkin, "Determination of optical properties of turbid media spanning visible and near-infrared regimes via spatially modulated quantitative spectroscopy," *J. Biomed. Opt.* **15**(1), 017012 (2010).
5. A. Garcia-Valenzuela, R. G. Barrera, and E. Guiterrez-Reyes, "Rigorous theoretical framework for particle sizing in theoretical colloids using light refraction," *Opt. Express* **16**(24), 19741–19756 (2008).
6. F. Martelli and G. Zaccanti, "Calibration of scattering and absorption properties of a diffusive liquid medium at NIR wavelengths: CW method," *Opt. Express* **15**(2), 486–500 (2007).
7. C. Chen et al., "A primary method for determination of optical parameters of turbid samples and application to intralipid between 550 and 1630 nm," *Opt. Express* **14**(16), 7420–7435 (2006).
8. H. Xu and M. Patterson, "Determination of the optical properties of tissue-simulating phantoms from interstitial frequency domain measurements of relative fluence and phase difference," *Opt. Express* **14**(14), 6485–6501 (2006).
9. S. Menon, Q. Su, and R. Grobe, "Determination of g and μ using multiply scattered light in turbid media," *Phys. Rev. Lett.* **94**(15), 153904 (2005).
10. A. Dimofte, J. Finlay, and T. Zhu, "A method for determination of the absorption and scattering properties interstitially in turbid media," *Phys. Med. Biol.* **50**(10), 2291–2311 (2005).
11. A. Reyes-Coronado et al., "Measurement of the effective refractive index of a turbid colloidal suspension using light refraction," *New J. Phys.* **7**(89), 1–22 (2005).
12. M. Gurfinkel, T. Pan, and E. Sevick-Muraca, "Determination of optical properties in semi-infinite turbid media using imaging measurements of frequency-domain photon migration obtained with an intensified charge-coupled device," *J. Biomed. Opt.* **9**(6), 1336–1346 (2004).
13. K. Yoshida et al., "Application of the critical angle method to refractive index measurement of human skin in vivo under partial contact," *J. Biomed. Opt.* **18**(3), 037002 (2013).
14. W. Guo et al., "A local curve-fitting method for the complex refractive index measurement of turbid media," *Meas. Sci. Tech.* **23**(4), 047001 (2012).
15. W. Guo et al., "A two-reflection divergent differentiating critical angle refractometer," *Rev. Sci. Instrum.* **82**(5), 053108 (2011).
16. W. Calhoun et al., "Measurement of the refractive index of highly turbid media," *Opt. Lett.* **35**(8), 1224–1226 (2010).
17. W. Calhoun et al., "Measurement of the refractive index of highly turbid media: reply to comment," *Opt. Lett.* **36**(16), 3172 (2011), and references therein.

18. W. Calhoun et al., "Sensitive real-time measurement of the refractive index and attenuation coefficient of milk and milk-cream mixtures," *J. Dairy Sci.* **93**(8), 3497–3504 (2010).
19. I. Niskanen, J. Räty, and K.-E. Peiponen, "Complex refractive index of turbid liquids," *Opt. Lett.* **32**(7), 862–864 (2007).
20. A. Garcia-Valenzuela et al., "Coherent reflection of light from a turbid suspension of particles in an internal-reflection configuration: theory vs. experiment," *Opt. Express* **13**(18), 6723–6737 (2005), and references therein.
21. G. Meeten and A. North, "Refractive index measurements of absorbing and turbid fluids by reflection near the critical angle," *Meas. Sci. Tech.* **6**(2), 214–221 (1995).
22. P. Di Ninni, F. Martelli, and G. Zaccanti, "Intralipid: towards a diffusive reference standard for optical tissue phantoms," *Phys. Med. Biol.* **56**(2), N21–N28 (2011), and references therein.
23. R. Michels, F. Foschum, and A. Kienle, "Optical properties of fat emulsions," *Opt. Express* **16**(8), 5907–5925 (2008).
24. J. Choukeife and J. L'Huillier, "Measurements of scattering effects within tissue-like media at two wavelengths of 632.8 nm and 680 nm," *Lasers Med. Sci.* **14**(4), 286–296 (1999).
25. S. Flock et al., "Optical properties of intralipid: a phantom medium for light propagation studies," *Lasers Surg. Med.* **12**(5), 510–519 (1992).
26. H. van Staveren et al., "Light scattering in intralipid-10% in the wavelength range of 400–1100 nm," *Appl. Opt.* **30**(31), 4507–4514 (1991).
27. I. Driver et al., "The optical properties of aqueous suspensions of intralipid, a fat emulsion," *Phys. Med. Biol.* **34**(12), 1927–1930 (1989).
28. D. F. Driscoll, "Lipid injectable emulsions: pharmacopeial and safety issues," *Pharm. Res.* **23**(9), 1959 (2006).
29. K. G. Goyal et al., "Refractive index sensing of turbid media by differentiation of the reflectance profile: does error-correction work?," *Rev. Sci. Instr.* **83**(8), 086107 (2012).
30. A. Ishimaru and Y. Kuga, "Attenuation constant of a coherent field in a dense distribution of particles," *J. Opt. Soc. Am.* **72**(10), 1317–1320 (1982).
31. M. McClimans et al., "Real-time differential refractometry without interferometry at a sensitivity level of 10^{-5}," *Appl. Opt.* **45**(25), 6477–6486 (2006).
32. A. Snyder and J. Love, "Goos-Hänchen shift," *Appl. Opt.* **15**, 236 (1976).
33. S. A. Prahl, "Mie scattering calculator," http://omlc.ogi.edu/calc/mie_calc.html (1998).
34. B. H. McGuyer, "Atomic physics with vapor-cell clocks," Ph.D. Dissertation, Princeton University (2012).
35. M. Boccard et al., "Light trapping in solar cells: analytical modeling," *Appl. Phys. Lett.* **101**(15), 151105 (2012).
36. P. P. Banerjee et al., "Binary nanoparticle dispersed metamaterial implementation and characterization," *Proc. SPIE* **8268**, 826805 (2012).
37. Z. Wu et al., "Plasmonic electro-optic modulator design using a resonant metal grating," *Opt. Lett.* **33**(6), 551–553 (2008).